Low-Frequency Modes of Tropical Ocean Dynamics*

FEI-FEI JIN

Department of Meteorology, School of Ocean and Earth Science and Technology, University of Hawaii at Manoa, Honolulu, Hawaii

(Manuscript received 24 October 2000, in final form 4 April 2001)

ABSTRACT

Basinwide very low-frequency (VLF) modes with zonal uniformly deepening and shoaling of the equatorial thermocline are found as solutions of linear shallow-water equations with the meridional basin boundaries under an equatorial β plane. They can be understood as the free heat-content recharge oscillations. The interannual VLF modes had been recognized as the essential part of the coupled recharge oscillator theory for the El Niño–Southern Oscillation. It is suggested that the decadal VLF modes may also be transformed into coupled modes relevant to the Pacific decadal climate variability through the ocean–atmosphere interaction in the Tropics.

1. Introduction

The great progress made in El Niño–Southern Oscillation (ENSO) theory (cf. Neelin et al. 1998) during the past two decades was built upon the foundation of tropical dynamics. Popular prototype models for understanding ENSO, such as delay-oscillator theory (Suarez and Schopf 1988; Battisti and Hirst 1989) and wave-oscillator theory (Cane et al. 1990), were all based on equatorial ocean wave dynamics. The more recently proposed recharge oscillator theory (Jin 1996, 1997a,b; Jin and An 1999) highlighted the slow dynamics of the equatorial heat content recharge/discharge and the associated variations in zonal-mean anomalous thermocline depth. However, the nature of this slow dynamics has not been fully explored.

Moreover, there is increasing interest in the research community on the origin of the decadal oscillations of the tropical Pacific. Although, not as strong as the ENSO signal, decadal variations in the Tropics and throughout the North Pacific as well as the entire globe have been identified from various data sources (cf. Latif 1998). There is also evidence of the decadal modulations of the frequency, amplitude, and predictability of ENSO. However, our understanding of the dynamics of decadal variability is still elusive with several competing proposed mechanisms remaining viable. Some of the theories focus on the midlatitude ocean–atmosphere interactions (Latif and Barnett 1994; Jin 1997c), whereas others invoke the ocean–atmosphere interactions of tropical and extratropical regions through both oceanic and/or atmosphere teleconnections (Gu and Philander 1997; Kleeman et al. 1999; Pierce et al. 2000; Jin et al. 2001). Decadal variability was also simulated in the Cane–Zebiak model (Cane and Zebiak 1985). It was pointed out recently that decadal variability in this model may be related to a specific nonlinear process (Timmermann and Jin 2001, manuscript submitted to *J. Climate*). There are also indications from coupled model simulations that the tropical ocean–atmosphere system alone may be one source of the decadal climate variability (Knutson and Manabe 1998; Yukimoto et al. 2000). Yet the existence of such long time scales in the tropical ocean dynamics has not been documented. Thus the possibility of the tropical origin of decadal variability is still far from thoroughly explored. In this paper, it is shown analytically that there exists a family of very low-frequency (VLF) modes in the tropical ocean dynamics. This is the first time that their nature is examined and their relevant decadal climate variability is discussed.

2. Low-frequency spectrum of the ocean dynamics

The upper-ocean dynamics of the tropical Pacific may be described by a shallow-water model. Under the long-wave approximation on the equatorial β plane, it can be written as (e.g., Cane and Sarachik 1981)

$$\begin{aligned}(\partial_t + \varepsilon_m)u - \beta y v + g'\partial_x h &= 0\\ \beta y u + g'\partial_y h &= 0\\ (\partial_t + \varepsilon_m)h + H(\partial_x u + \partial_y v) &= 0,\end{aligned} \tag{1}$$

where u and v are the zonal and meridional ocean cur-

* School of Ocean and Earth Science and Technology Contribution Number 5671.

Corresponding author address: Prof. Fei-Fei Jin, Department of Meteorology, School of Ocean and Earth Science Technology, University of Hawaii at Manoa, 2525 Correa Rd., Honolulu, HI 96822-2219.
E-mail: jff@soest.hawaii.edu

rents, h is the departure of the upper-layer thickness from the reference depth H (150 m) and represents a thermocline depth anomaly field, and g' is the reduced gravity parameter that gives rise to an internal gravity speed as $c_0 = \sqrt{g'H} = 2.7$ m s^{-1}. The boundary conditions for the shallow-water equations in the long-wave approximation are used:

$$u(L, y, t) = 0, \qquad \int_{-\infty}^{\infty} u(0, y, t)\, dy = 0. \tag{2}$$

System (1) can be nondimensionalized by the oceanic Rossby deformation radius $L_0 = \sqrt{c_0/\beta}$ for y, the ocean basin width L for x, the Kelvin wave crossing time L/c_0 (set as 2 months) for t, the reference depth H for h, the Kelvin wave speed c_0 and c_0L_0/L for u and v, respectively. Two new variables q and p are used to replace the nondimensionalized u and h by setting $q = h + u$, and $p = h - u$. Expanding q, p in terms of hyperbolic cylinder functions $\{\psi_{2n}(y), n = 0, 1, 2, \ldots\}$ (cf. Battisti 1988), and considering only hemispheric symmetric solutions, one can obtain the following wave equations:

$$(\partial_t + \epsilon_m)q_{2n} - \partial_x q_{2n}/(4n - 1) = 0 \tag{3}$$

with $n = 0$ for Kelvin wave and $n = 1, 2, 3\ldots$ for the first, second, and third symmetric Rossby waves. The boundary conditions to determine the reflections among the Kelvin and Rossby waves at east and west boundaries now can be written as

$$q_{2n+1}(x = 1, t) = q_{2n-1}(x = 1, t)\sqrt{(2n - 1)/2n}, \qquad n = 1, 2, 3 \ldots$$

$$q_0(x = 0, t) = \sum_{n=1}^{N} \frac{d_{2(n-1)}}{(2n(2n - 1))^{1/2}} q_{2n-1}(x = 0, t)$$

$$d_{2n} = ((2n)!)^{1/2}/(2^n n!). \tag{4}$$

Assuming an eigensolution:

$$q_{2n} = B_n \exp((\sigma + \varepsilon_m)(4n(x - 1) - x + t) - \varepsilon_m t) \tag{5}$$

and using Eq. (4), the eigenvalue equation for a truncation at N symmetric Rossby waves can be written as

$$1 - \sum_{n=1}^{N} \frac{(2n - 3)!!}{(2n)!!} z^n = 0, \qquad z = \exp(-4\sigma). \tag{6}$$

Here $(2n)!! = 2 \cdot 4 \cdot 6 \cdot \cdots \cdot 2n$, and $(-1)!! = 1$. It should be noted that in the eigensolution (5) σ is the eigenvalue without the linear damping whereas the effect of the linear damping ε_m is separately included in the solution (5). As shown in Neelin and Jin (1993), there are N solutions of z with z_j as the roots of the Nth-order polynomial equation. With sufficiently high truncation, the roots are almost equally distributed just outside of the unit circle on the complex plane of z (Neelin and Jin 1993). They can also be approximately expressed as

$$z_j = \rho_j \exp(ij2\pi/N), \qquad j = 0, 1, \ldots, N - 1. \tag{7}$$

Thus the eigenvalues can be expressed approximately as

$$\sigma_{j,k} = (-(\ln\rho_j - ij2\pi/N) \pm ik2\pi)/4, \qquad j = 0, 1, \ldots, N - 1; \qquad k = 0, 1, 2, \ldots, \tag{8}$$

and the corresponding eigen structures are

$$q_{j,k}(x, y, t) = \sum_{n=0}^{N} q_{2n}^{j,k}(x, t)\psi_{2n}(y)$$

$$p_{j,k}(x, y, t) = \sum_{n=0}^{N-1} p_{2n}^{j,k}(x, t)\psi_{2n}(y)$$

$$q_{2n}^{j,k} = \sqrt{(2n - 1)!!/(2n)!!} \times \exp\{\sigma_{j,k}[4n(x - 1) - x + t] - \varepsilon_m t\},$$

$$p_{2n}^{j,k} = \sqrt{(2n + 2)/(2n + 1)}\, q_{2n+2}^{j,k}, \tag{9}$$

where k is the node number of the eigenfunction in the zonal direction near the equator. All $\ln\rho_j$ are positive, indicating the eigenmodes are all damped. From this point on, we will also set $\varepsilon_m = 0$. In this case, damping rates of the these modes only come from two sources: the finite truncations, and the energy loss of the system at the western boundary due to the long-wave approximation even without truncation (Jin 1997b). The damping rates of all modes become small as the truncation N becomes very large. For $N = 101$, the highest damping rate is about 0.06, which is corresponding to an e-folding time of about 2.5 yr. This damping rate can be further cut to about half if the truncation is doubled. The long-wave approximation in some sense can be viewed as instantly removing all the reflected short Rossby waves with eastward propagation group velocity. Thus energy is continuously lost in the western boundary under the long-wave approximation.

When $N \to \infty$ and there is a root $z_0 = 1$, $\sigma_{0,k} = \pm(ik2\pi)/4$ ($k = 1, 2, 3, \ldots$) and corresponds to the so-called ocean basin modes (Cane and Moore 1981). All these modes are undamped because they automatically satisfy the no-normal-flow boundary conditions and thus conserve their energy (Jin 1997b). The gravest ocean basin mode has the lowest frequency of $\pi/2$, which corresponds to a period about 8 months. The case of $\sigma_{0,0} = 0$ is the so-called ''trivial solution'' with $h =$ constant, $u = 0$, and $v = 0$.

For any finite N, the real and imaginary parts of the eigenvalues can be plotted as the functions of the pseudowavenumbers defined as $k_j = k + j/N$ ($k = 0, 1, 2, \ldots$, and $j = 0, 1, 2, \ldots, N$). The results are shown in Fig. 1. The modes found by Cane and Moore now correspond to the least damped modes with $j = 0$ in the truncated case (so $k_j = 0, 1, 2, \ldots$, as indicated by the heavy dots in Fig. 1). However, the modes found by Cane and Moore, the undamped modes, are only a small part of the complete and almost continuous spectrum of the system (1) under the boundary condition (2). The modes near the zero frequency are called VLF modes ($k = 0$, $j \ll N$). This class of modes was implicitly

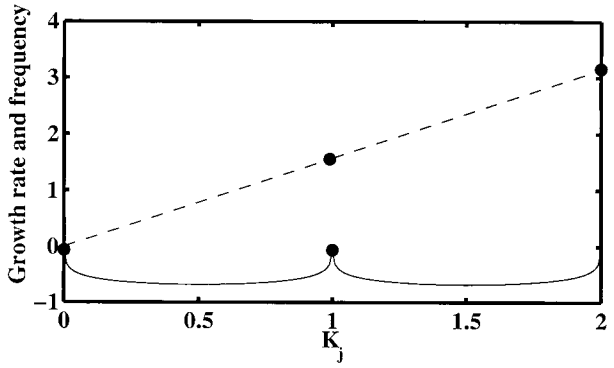

FIG. 1. The eigenvalue distribution with respect to the index $k_j = k + j/N$. The straight line is the dependence of the imaginary part (frequency) of the eigenvalue on k_j and the curve is the dependence of the real part (growth rate) of the eigenvalues on k_j. The real part is multiplied by 10 to display its variations more clearly. Heavy dots indicate the eigenvalues for the ocean basin modes ($k_j = 0, 1, 2, \ldots$).

included in the solutions of Moore (1968); however, the nature of these VLF modes has not been examined.

3. Structure of the VLF modes

For the modes in the vicinity of the gravest ocean basin mode ($k = 1$, $j = 0$), their structures are similar to the gravest ocean basin modes, which have a node in the equatorial thermocline, and to the patterns shown in Cane and Moore (1981) as shown in Fig. 2a. In contrast, the VLF modes show zonal uniformly deepening and shoaling of the equatorial thermocline as shown in Figs. 2b and 2c. These vacillations in the equatorial thermocline are associated with the slow westward progression of the off-equatorial Rossby waves. They are continuously reflected into the equatorial Kelvin wave so that it has sufficient strength to satisfy the western boundary condition, whereas the Kelvin wave then continuously generates Rossby waves at the eastern boundary to meet the eastern boundary conditions. Since the time L/c_0 for basin-crossing time of the Kelvin wave is set as 2 months (which is thus the unit for the nondimensional time), the period of the gravest ocean basin mode ($j = 0$, $k = 1$, thus $k_j = 1$) is about 8 months, whereas the periods for the VLF modes shown ($k = 0$, $j = 15$ and 5, the pseudowavenumber k_j is about 0.15 and 0.04, respectively) are about 4 and 14 yr with the decay rates about 3–4 yr. Although the basin-crossing times for the Kelvin wave and the first symmetric Rossby wave are only 2 and 6 months, respectively, the long periods of the VLF modes are possible because of the heavy participation of the slow off-equatorial Rossby waves as shown in Figs. 3–6. It also should be mentioned that the small real part of the eigenvalue in the eigensolution (9) is suppressed in calculating the eigenstructures shown in Figs. 2–6. Suppressing the damping rates of these modes removes not only the decay of the amplitudes but also small-scale features in the thermocline field. These small-scale features would otherwise be rather strong particularly in the western part of the basin away from the equatorial region, and they are related to the leak of the energy of the system as well as the finite truncations.

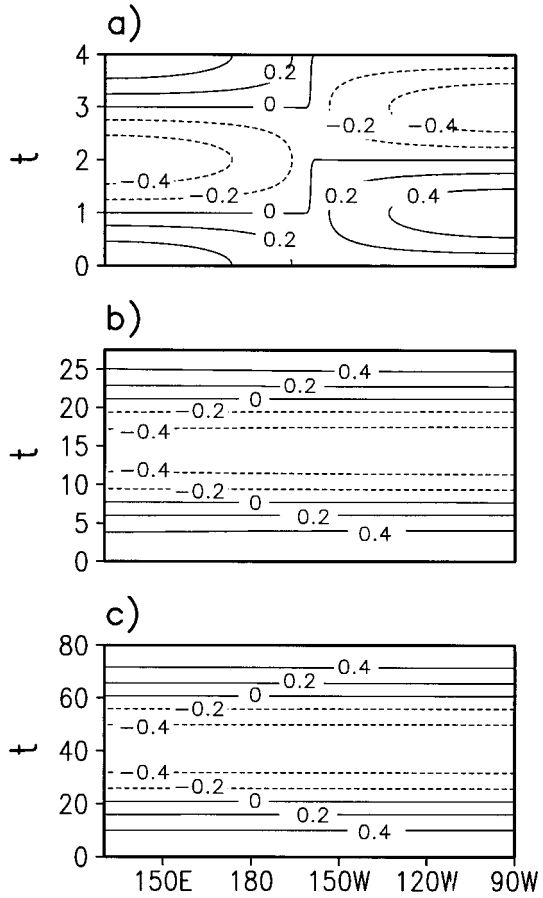

FIG. 2. The thermocline along the equator over one period for the solutions (a) $k_j = 1$ ($k = 1$, $j = 0$), (b) $k_j = 0.14$ ($k = 0$, $j = 15$), and (c) $k_j = 0.04$ ($k = 0$, $j = 5$). The truncation number N is 101.

4. VLF modes as free recharge oscillation and implications

It is rather difficult to visually relate the oscillation of the equatorial thermocline shown in Figs. 3 and 5 to the reflection of Rossby wave packets because of the broad participation of the Rossby waves at various latitudes. It is easier to examine the slope of the thermocline field and the meridional velocity field in the off-equatorial region and then to relate them to the associated recharge/discharge of the equatorial thermocline through the oscillation. For instance, at the maximum phase and outside of the relative uniform equatorial thermocline anomaly (Fig. 3a), there is a clear zonal slope in this latitude band about 5°–10°N, whereas at higher latitudes, the thermocline slope alternates

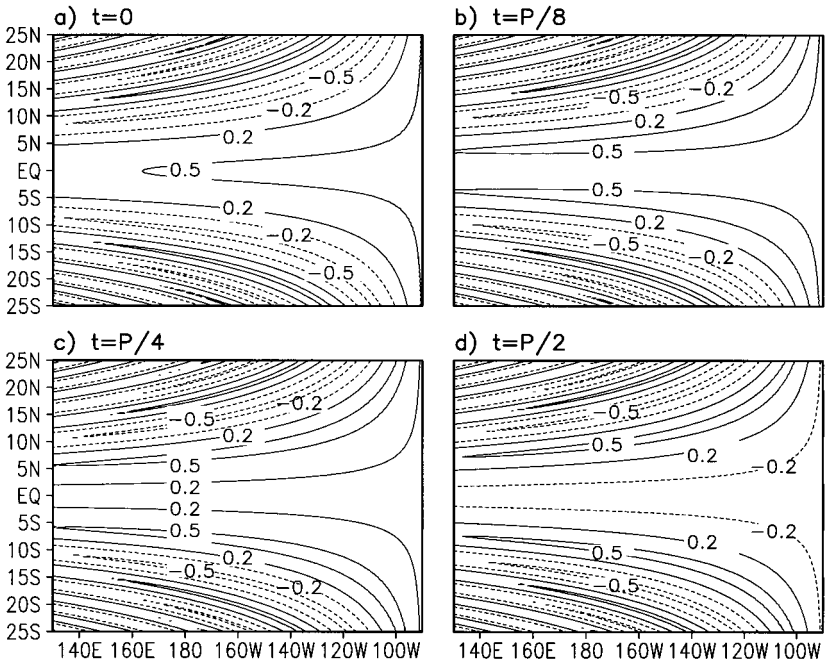

FIG. 3. The thermocline of the solution in Fig. 2b ($k_j = 0.14$) at the different phases of the oscillation throughout a half period.

crossing the basin in the zonal direction. The slope of the thermocline in the latitude band adjacent to the equatorial region indicates a strong net meridional transport of mass out of the equatorial region, or discharge of the equatorial heat content due to the Rossby wave activity in the effective latitude band, whereas alternating slopes at the higher latitude result in little net meridional transport cross the whole basin. It is the discharge process in this effective latitude band next to the equatorial waveguide that causes the shoaling of the equatorial thermocline and makes the positive equatorial thermocline anomaly diminish at the transition phase (Fig. 3c). At this time, the sign of the major part of the zonal slope still remains, and thus the equatorial thermocline goes on to the negative phase (Fig. 3d). At this phase, the slope is already reversed in the effective latitude band and the recharge process has already begun; this will bring the equatorial thermocline back to the maximum phase. The above recharge/discharge of the equatorial heat content can be more directly seen from the meridional velocity field as show in Fig. 4. Therefore, the deepening and shoaling of the equatorial thermocline associated with the VLF mode can be understood as a natural free recharge oscillation.

The nearly zonal uniform shoaling and deepening of the near-equatorial thermocline is the unique feature of the VLF modes, which is of great significance in understanding the low-frequency thermocline climate variation in the equatorial region. It is known that associated with ENSO, the basinwide height difference of the equatorial thermocline is always in quasi-equilibrium with the zonally integrated wind stress, whereas the zonal mean of the equatorial thermocline anomaly lags behind the wind stress forcing by about a year. In fact, even in an uncoupled but periodic forced solution of the system (1), Cane and Sarachik (1981) analytically found that there are also two parts in the thermocline solution under zonal uniform wind stress forcing. One is the east–west thermocline contrast along the equator that is in balance with the stress, whereas the other part, a constant equatorial thermocline, almost always has a significant phase lag behind the forcing. The second part of the solution, similar to the part of zonally uniform thermocline anomaly in the coupled ENSO mode, can be viewed as the excitation of the VLF modes of the tropical ocean dynamics. The fact that the zonal mean of equatorial thermocline anomalies is not in quasi balance with equatorial zonal wind stress anomalies and its implication to ENSO dynamics were already recognized by Cane (1992). This phase lag, namely, the zonal means of equatorial thermocline anomalies lag behind the equatorial zonal wind stress anomalies, was later demonstrated as critical for the phase transition of the ENSO and is at the heart of the coupled recharge oscillator paradigm of ENSO (Jin 1996, 1997a,b; Jin and An 1999).

The shoaling and deepening of the nearly zonal uniform thermocline associated with the VLF modes is essentially related to the equatorial ocean heat content recharge and discharge. The coupled recharge oscillator theory for ENSO had its foundation in the slow dynamics of the tropical ocean dynamics. It was found by Jin and Neelin (1993) and more recently in van der Vaart et al. (2000) that the unique ENSO-like coupled mode

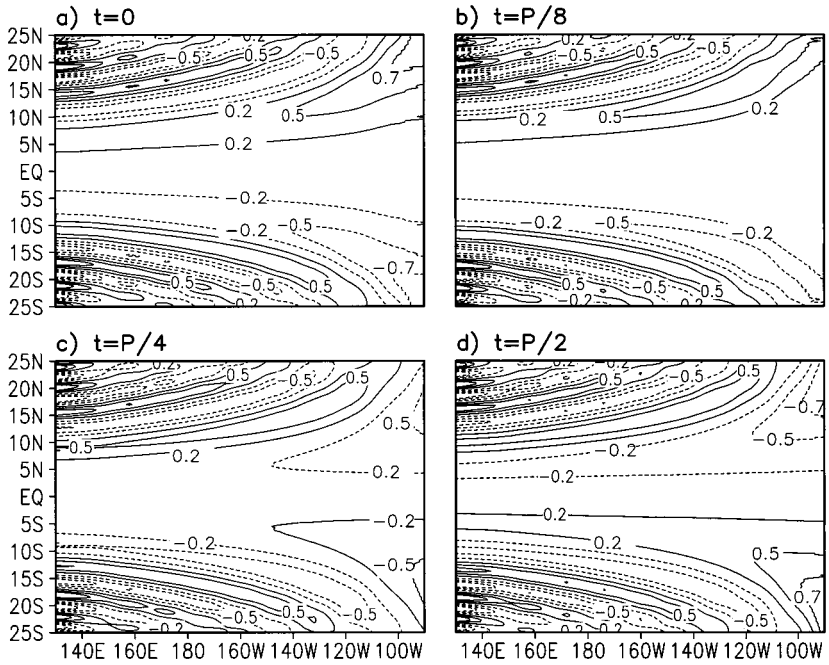

FIG. 4. The meridional velocity of the solution in Fig. 2b ($k_j = 0.14$) at the different phases of the oscillation throughout a half period. It should be noted that if the dimensional unit for the thermocline field shown in Fig. 3 is in units of H, then the meridional velocity is in units of c_0L_0/L.

arises from the low-frequency spectrum of ocean dynamics. In the coupled mode, the structure of the thermocline field undergoes dramatic changes because of the participation of the wind stress that is related to SST variations of the coupled mode. The thermocline of the coupled ENSO mode also has two important parts, that is, the east–west contrast along the equator and zonally uniform anomaly near the equator. The east–west difference in the thermocline anomaly is in quasi balance with the zonal wind stress and is thus always nearly in phase with the SST field of the coupled mode. It has been well known that this part of thermocline anomaly has its peak phase near the peak phase of SST anomaly. It reinforces the SST anomaly and makes the coupled mode grow. The zonally uniform anomaly near the equator in the thermocline field lags the SST anomalies about a quarter cycle and thus becomes clear at the transition phases of the SST field of the coupled ENSO mode. Moreover, at these phases of the coupled mode, there is little wind anomaly and thus little zonal contrast of the equatorial thermocline anomaly. In the coupled recharge oscillator theory (Jin 1997a,b), the phase lag of the equatorial zonal mean thermocline and the equatorial zonal wind stress is the essential feature for understanding the phase transition and is explained by recharge/discharge of the equatorial heat content resulted from the Rossby wave activity in the neighborhood of the equatorial waveguide. The effective latitude bands of the Rossby activity in the near-4-yr VLF mode and the coupled ENSO mode are the same. This is not a coincidence, but rather indicates a selection mechanism for a free mode to be transformed into the coupled ENSO mode with a 4-yr periodicity. The effective latitude band in the coupled mode is controlled by the meridional scale of SST anomaly and the associated wind stress. This scale is set by the coupled processes and the climatological state of the tropical system. It also should be pointed out that in addition to the meridional scale of the coupled mode, its periodicity may also depend on other details, such as the longitudinal distributions of the mode as well.

The VLF modes on the decadal timescale shown in Figs. 5 and 6 can be understood as an even slower recharge oscillator in the same manner as the mode on the interannual timescale shown in Figs. 3 and 4. The only difference between the interannual and decadal modes is the location of the effective latitude bands of the recharge/discharge of the equatorial heat content by the Rossby wave activity. For the decadal modes, the effective latitude band is at a relatively higher latitude about 10°–20° from the equator. This dependence of the effective latitude bands of the recharge/discharge of the equatorial heat content on the frequencies of the VLF modes is shown most clearly in Fig. 7. In this plot, we use the meridional velocity at $x = 1/2$ as the indication of recharge and discharge of the equatorial heat content because this field has nearly uniform sign in low latitudes within one side of the equator. A nondimensional frequency of 0.25 corresponds to a period of about 50 months (the dimensional periods are 2π divided by the nondimensional frequencies, with units of 2 months). It becomes clear that the effective latitudes for equatorial

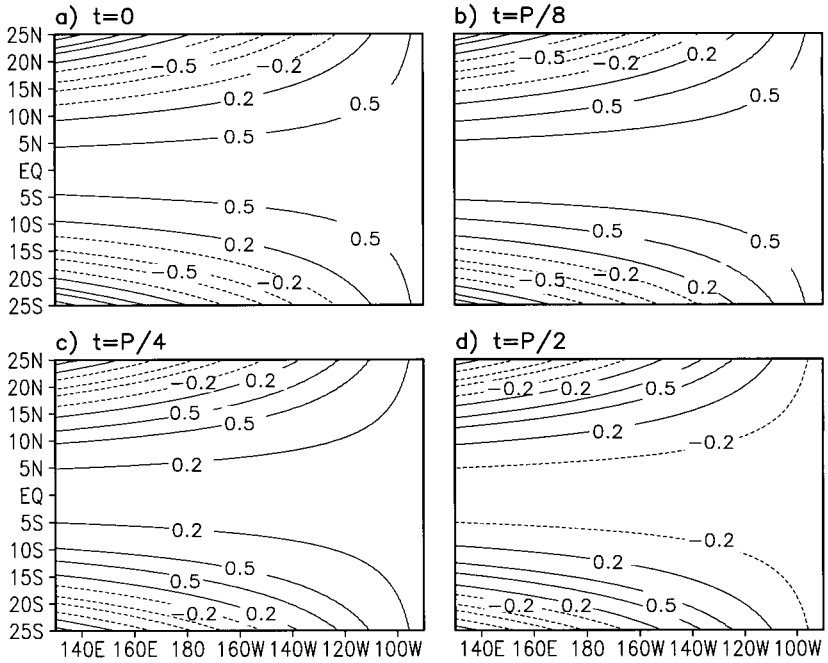

FIG. 5. The same as in Fig. 3 except for solution in Fig. 2c ($k_j = 0.04$).

heat content recharge/discharge are significantly different for different frequencies. Rossby wave activity in the region of 10°–20° from the equator has been suggested as the oceanic bridge between the midlatitudes and equatorial region for the climate variability on the decadal timescale (e.g., Jin et al. 2001). The effectiveness of Rossby wave activity in the region in altering equatorial thermocline on the decadal timescale as shown in Figs. 5–7 tends to support the argument.

Although the interannual VLF modes had been recognized as the essential part of the coupled recharge oscillator theory for the El Niño–Southern Oscillation (ENSO), the relevance of the decadal VLF modes revealed is not clearly demonstrated. The existence of the

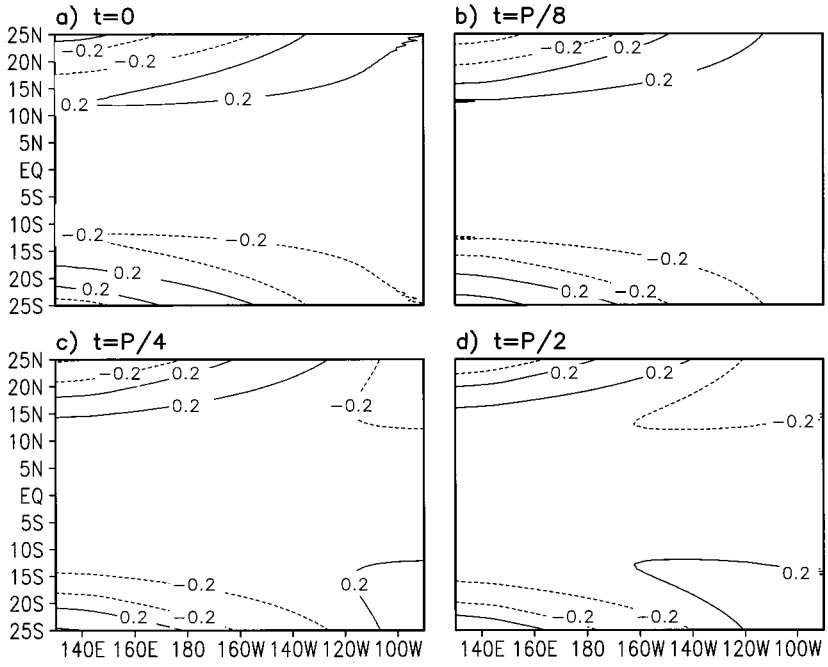

FIG. 6. The same as in Fig. 4 except for solution in Fig. 2c ($k_j = 0.04$).

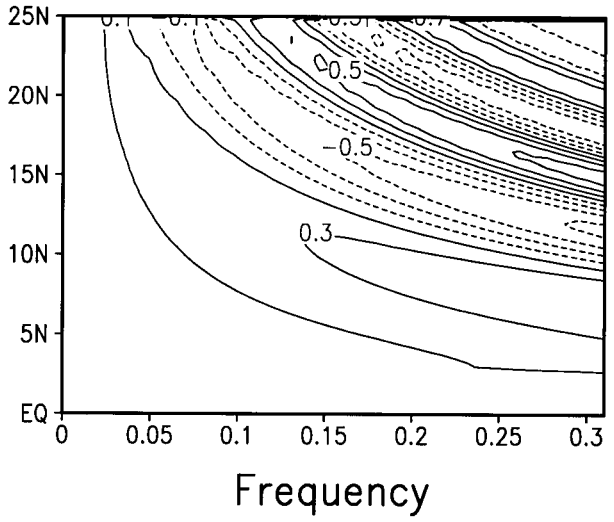

FIG. 7. The distribution of meridional velocity at $x = 1/2$ for each low-frequency mode at the maximum phase of the equatorial thermocline.

VLF modes on the decadal timescale provides a possible mechanism for the decadal climate variability in the tropical–subtropical regions, although the coupled processes to form coherent decadal variability need to be more clearly demonstrated. The decadal oscillations in recent coupled GCM simulations (Knutson and Manabe 1998; Yukimoto et al. 2000) were found to have dynamical features similar to the ENSO mode. It was therefore speculated that the simulated decadal mode might be interpreted by a mechanism similar to that for ENSO. The VLF modes found in this study may provide the needed dynamical foundation for substantiating this speculation. There are good reasons that the decadal VLF mode can transform itself through atmosphere–ocean interaction in the Tropics and subtropics to a coupled mode related to the observed decadal climate variability in the Pacific. First, the effective latitudes for initiating substantial equatorial decadal thermocline variability lie around the subtropical regions (about 15°–20° from the equator). Second, the decadal SST patterns in the Tropics are of wider meridional scale than that of SST patterns of ENSO, thus a great portion of wind stress curl associated with this decadal SST can be located in the effective latitude band. We have found that if we add into Eq. (1) a specified hemispheric wind stress pattern in this band with its amplitude coupled with the thermocline fluctuation in the eastern tropical Pacific, a coupled decadal mode is indeed generated from the VLF spectrum in a similar manner as the ENSO mode through tropical and subtropical ocean–atmosphere interaction. We also have found both damped and self-sustained coupled decadal modes in this simple coupled model for different strengths of coupling. The detailed analysis of this kind of coupled mode will be reported separately.

5. Conclusions

In this paper, a family of VLF modes of tropical ocean dynamics was revealed and their nature is examined. These VLF modes share a common feature in the oscillations of nearly zonal uniform thermocline in the equatorial region. The oscillations of the nearly zonal uniform equatorial thermocline of these VLF modes can be understood as the recharge/discharge of the equatorial heat content due to the off-equatorial Rossby wave packets. The coupled recharge oscillator that serves as a simple model for ENSO is closely related to the free recharge oscillations on the similar timescale.

Moreover, decadal timescale oscillations of the equatorial zonal mean heat content associated with the ocean adjustment mode of the tropical ocean dynamics have essentially the same physical nature as that of the interannual modes. The effective latitudes of Rossby wave activity for the interannual modes on the ENSO timescale are in the neighborhood of the equatorial region, whereas for the decadal modes, the effective latitudes are moved toward the subtropics. It is thus suggested that a coupled mode of similar physics as the ENSO mode on the decadal timescale, whose existence was speculated in recent coupled GCMs (Knutson and Manabe 1998; Yukimoto et al. 2000), is indeed plausible. Further work to demonstrate its relevance to the decadal climate variability in the Pacific and decadal modulations of ENSO is still under active research.

Acknowledgments. This work was supported by National Science Foundation Grant ATM-956152 and by National Oceanographic and Atmospheric Administration Grant GC97234. It was largely completed when the author was on his sabbatical leave visiting CCSR of Tokyo University. The author is grateful to Prof. Mark Cane and another anonymous reviewer for their thoughtful and helpful comments; to Lin-Lin Pan, who did all the calculations and graphics; and to Diane Henderson and Jingxia Zhao for editing the manuscript.

REFERENCES

Battisti, D. S., 1988: The dynamics and thermodynamics of a warming event in a coupled tropical atmosphere/ocean model. *J. Atmos. Sci.,* **45,** 2889–2919.

——, and A. C. Hirst, 1989: Interannual variability in the tropical atmosphere/ocean system: Influence of the basic state and ocean geometry. *J. Atmos. Sci.,* **46,** 1687–1712.

Cane, M. A., 1992: A note on the fast wave limit and interannual oscillations. *J. Atmos. Sci.,* **49,** 1947–1949.

——, and D. W. Moore, 1981: A note on low-frequency equatorial basin modes. *J. Phys. Oceanogr.,* **11,** 1578–1584.

——, and E. S. Sarachik, 1981: The response of a linear baroclinic equatorial ocean to periodic forcing. *J. Mar. Res.,* **39,** 651–693.

——, and S. Zebiak, 1985: A theory for El Niño and Southern Oscillation. *Science,* **222,** 1189–1194.

——, M. Münnich, and S. E. Zebiak, 1990: A study of self-excited oscillations of the tropical ocean–atmosphere system. Part I: Linear analysis. *J. Atmos. Sci.,* **47,** 1562–1577.

Gu, D., and S. G. H. Philander, 1997: Interdecadal climate fluctuations

that depend on exchanges between the tropics and extratropics. *Science,* **275,** 805–807.
Jin, F.-F., 1996: Tropical ocean–atmosphere interaction, the Pacific cold tongue, and the El Niño Southern Oscillation. *Science,* **274,** 76–78.
——, 1997a: An equatorial ocean recharge paradigm for ENSO. Part I: Conceptual model. *J. Atmos. Sci.,* **54,** 811–829.
——, 1997b: An equatorial ocean recharge paradigm for ENSO. Part II: A stripped-down coupled model. *J. Atmos. Sci.,* **54,** 830–847.
——, 1997c: A theory of interdecadal climate variability of the North Pacific ocean–atmosphere system. *J. Climate,* **10,** 1821–1834.
——, and J. D. Neelin, 1993: Modes of interannual tropical ocean–atmosphere interaction—A unified view. Part I: Numerical results. *J. Atmos. Sci.,* **50,** 3477–3502.
——, and S.-I. An, 1999: Thermocline and zonal advective feedbacks within the equatorial ocean recharge oscillator model for ENSO. *Geophys. Res. Lett.,* **26,** 2989–2992.
——, M. Kimoto, and X.-C. Wang, 2001: Decadal extratropical-tropical ocean–atmosphere interaction and its modulation on ENSO. *Geophys. Res. Lett.,* **28,** 1531–1534.
Kleeman, R., J. P. McCreary, and B. A. Klinger, 1999: A mechanism for generating ENSO decadal variability. *Geophys. Res. Lett.,* **26,** 1743–1746.
Knutson, T. R., and S. Manabe, 1998: Model assessment of decadal variability and trends in the tropical Pacific Ocean. *J. Climate,* **11,** 2273–2296.
Latif, M., 1998: Dynamics of interdecadal variability in coupled ocean–atmosphere models. *J. Climate,* **11,** 602–624.
——, and T. P. Barnett, 1994: Causes of decadal climate variability over the North Pacific and North America. *Science,* **266,** 634–637.
Moore, D. W., 1968: Planetary-gravity waves in an equatorial ocean. Ph.D. thesis, Harvard University, Cambridge, MA, 207 pp.
Neelin, J. D., and F.-F. Jin, 1993: Modes of interannual tropical ocean–atmosphere interaction—A unified view. Part II: Analytical results in the weak-coupling limit. *J. Atmos. Sci.,* **50,** 3504–3522.
——, D. S. Battisti, A. C. Hirst, F.-F. Jin, Y. Wakata, T. Yamagata, and S. E. Zebiak, 1998: ENSO theory. *J. Geophys. Res.,* **103** (C7), 14 261–14 292.
Pierce, D. W., T. P. Barnett, and M. Latif, 2000: Connections between the Pacific Ocean Tropics and midlatitudes on decadal timescales. *J. Climate,* **13,** 1173–1194.
Suarez, M. J., and P. S. Schopf, 1988: A delayed action oscillator for ENSO. *J. Atmos. Sci.,* **45,** 3283–3287.
Timmermann, A., and F.-F. Jin, 2001: A nonlinear mechanism of decadal amplitude modulation of ENSO and its predictability. *J. Climate*, submitted.
van der Vaart, P. C., H. Dijkstra, and F.-F. Jin, 2000: The Pacific cold tongue and the ENSO mode: A unified theory within the Zebiak–Cane model. *J. Atmos. Sci.,* **57,** 967–988.
Yukimoto, S., M. Endoh, and A. Noda, 2000: ENSO-like interdecadal variability in the Pacific Ocean as simulated in a coupled general circulation model. *J. Geophys. Res.,* **105,** 13 945–13 963.